

New Actuator System using Movable Pulley for Bio-mimetic System and Wearable Robot Applications

Hoyul Lee, Chulwoo Lee, Seongjin Kim, and Youngjin Choi

Abstract— This paper proposes a new actuator system using a movable pulley for a bio-mimetic system and wearable robot applications, which is able to store energy in advance and to release it in such a way to satisfy desired speed and force control performances, simultaneously. Since new actuator system consists of two motors (dual-motors), a movable pulley, and series spring connection for high speed/force operation characteristics, it is referred to as Dual-motor system using a Movable Pulley with a Series Elastic Actuator (DuMP-SEA) in this paper. Also, the proposed actuator system not only combines individual speed/force operation region of each motor, but also extends the combined operation region by using the energy stored in advance. Finally, we suggest the extended operation region (high speed and high force characteristics) obtained by using the DuMP-SEA through simulations and experiments.

I. INTRODUCTION

Bio-mimetic system and wearable robots have been actively researched as important fields of the robotic applications[1][2][3][4]. In detail, most wearable robots are researched for a military application and a power-assistive robotic application for a heavy worker and the disabled. The wearable robots should have some issues; light weight, compact size, operation safety, and portability for everyday life applications. For this, it is necessary to develop a small-sized, light-weighted, and safety-assured actuator system with high speed and high force capabilities. Hitt *et al.* have used a series elastic actuator (SEA) in designing a robotic device for a power assistance of human's ankle while human walking in [1]. They have designed the actuation mechanism with reducing the size of the required motor, by which energy is stored in the spring in advance and released when required to use. Moreover, the SEA system is able to contact softly to the environmental components including human [1-8].

It is important to select an actuator specification when a robot is designed. Indeed, the actuator speed and force (in this paper, a force implies a generalized force including torque) capabilities are dependent on the selection of motor and gear

ratio. For instance, if we select a large gear ratio with motor, the speed is reduced and force increases. On the contrary, if we select a small gear ratio with motor, the torque is reduced and the speed increases. Thus, if we want an actuator that provides both large force and high speed, it might be very difficult to make the small-sized actuator system without storing energy in advance and releasing it when required. Though the gear-transmission mechanism in an automobile has been used to change speed-force characteristics, it is not an appropriate alternative for wearable robots and rehabilitation robot due to its size and cost issues.

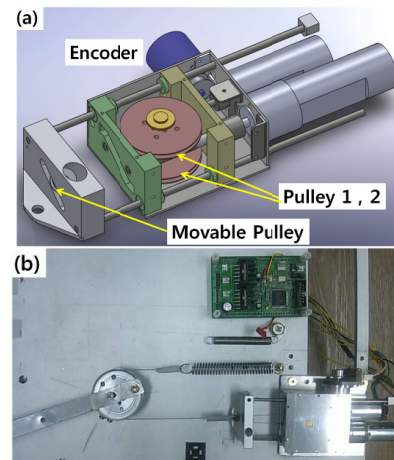


Fig. 1. Prototype of actuator, (a) Dual-motors system using a Movable Pulley (DuMP) (b) 1-DOF Series Elastic Actuator (SEA) with DuMP.

In this paper, a dual-motors system using a movable pulley (DuMP) is proposed as shown in Fig. 1 (a). Here, two motors have a role to supply both a large driving force and high speed capabilities to new actuator system; the one is used for the large force and the other for high speed. Also, the proposed system has a simple mechanical structure and its speed-force characteristic is obtained as a form which is combined using two motors with different objectives (high speed and large force). Ultimately, this paper suggests new actuator system by applying new Dual-motors system using a Movable Pulley (DuMP) to a conventional Series Elastic Actuator (SEA), and demonstrates its validity through experiments under various conditions.

II. NEW ACTUATOR SYSTEM

A. 1 DOF system using SEA

Let us consider 1-DOF planner series elastic actuator (SEA) system as shown in Fig. 2. First, the equivalent dynamic

This work was supported in part by the Korea Science and Engineering Foundation (KOSEF) grant funded by the Korea government (MEST) (R01-2008-000-20631), and in part by the Ministry of Knowledge Economy (MKE) and Korea Industrial Technology Foundation (KOTEF) through the Human Resource Training Project for Strategic Technology, Republic of Korea.

The authors are with the Department of Electronic, Electrical, Control and Instrumentation Engineering, Hanyang University, Republic of Korea. E-mail: cyj@hanyang.ac.kr

components of Fig. 2 can be redrawn as shown in Fig. 3. Indeed, Fig. 3 is a spring-mass model which is written as:

$$\mathbf{F} = \mathbf{M}\ddot{\mathbf{x}} = \mathbf{F}_s - \mathbf{F}_{\text{dist}}, \quad (1)$$

$$\mathbf{F}_s = \mathbf{k}(\mathbf{L} - \mathbf{x} - \mathbf{s}_0), \quad (2)$$

where \mathbf{x} denotes a position of the mass (or the displacement of liner actuator), \mathbf{F}_s is a spring force with spring coefficient \mathbf{k} , \mathbf{s}_0 is a free length of the spring, and \mathbf{F}_{dist} is a disturbance force. For simplicity, a gravitational force is neglected through the paper. Hence, an acceleration of the mass is obtained as follows:

$$\ddot{\mathbf{x}} = \frac{1}{\mathbf{M}} \{ \mathbf{k}(\mathbf{L} - \mathbf{x} - \mathbf{s}_0) - \mathbf{F}_{\text{dist}} \} \quad (3)$$

Since the liner actuator is composed of a pulley and a tendon wire, we should notice that the displacement of linear actuator may not be equal to the position of the mass if the wire can be freely released without the tension. Thus, we add an assumption that the tendon wire in the linear actuator is operated with an appropriate tendon force.

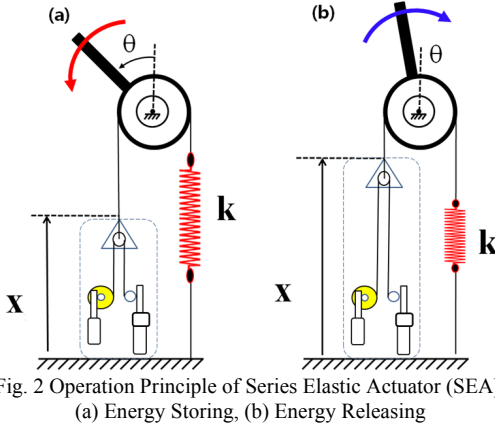


Fig. 2 Operation Principle of Series Elastic Actuator (SEA). (a) Energy Storing, (b) Energy Releasing

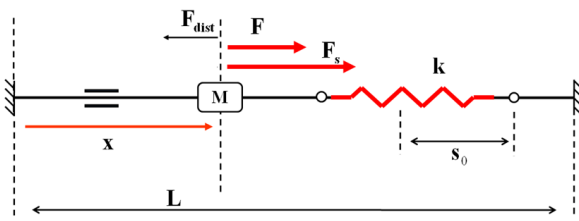


Fig.3 Spring-Mass Model

Second, according as linear actuator is operated, the corresponding spring force is changed as shown in Fig. 3. For instance, if the actuator displacement is reduced, then the energy is stored in the spring by increasing the spring force. On the contrary, if the actuator displacement is gradually enlarged, then the energy is released in the spring by decreasing the spring force. Also, if the spring force is larger than the disturbance force, then we can neglect \mathbf{F}_{dist} in Eq. (3). Thus, the inertial force of \mathbf{M} becomes equal to the spring force stored in the spring. This spring force can make fast motion by using the energy stored in the spring. This is one of the main advantages obtained by using SEA system. However,

to realize the SEA system with high performance, the linear actuator must have the following three conditions; the one is to store energy as fast as possible, another is to store energy as large as possible, and the other is to release energy in a wanted way in terms of desired speed and desired force. The following section will suggest new linear actuator system to satisfy above three conditions.

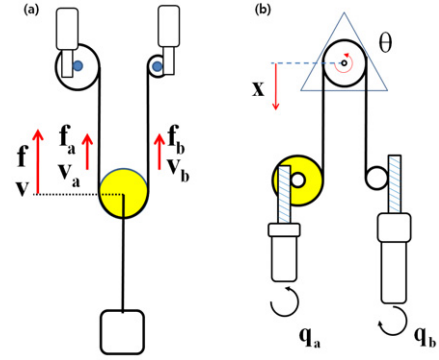


Fig.4. Concept of Dual-motors system using a Movable Pulley

B. Characteristic of the DuMP

In this section, we propose a new actuator system referred to as a Dual-motors system using a Movable Pulley, in short, DuMP, as shown in Fig. 4. The suggested DuMP improves the speed-force performance by making two motors operate in one movable pulley. Fig. 4(a) illustrates the concept of the DuMP, in which \mathbf{f}_a , \mathbf{f}_b denote the applied input forces of each motor, and \mathbf{v}_a , \mathbf{v}_b the applied input velocities of each motor, and \mathbf{f} , \mathbf{v} denote the output force and the output velocity of the movable pulley, respectively.

To obtain the relationship between input and output at the movable pulley system, let us consider the works done by each motor as follows:

$$\mathbf{w}_a = \mathbf{f}_a \delta \mathbf{x}_a, \quad (4)$$

$$\mathbf{w}_b = \mathbf{f}_b \delta \mathbf{x}_b,$$

where $\delta \mathbf{x}_a$ and $\delta \mathbf{x}_b$ imply the infinitesimal displacements of each motor, respectively. Also, the infinitesimal displacement of the pulley, $\delta \mathbf{x}$, is described as

$$\delta \mathbf{x} = \frac{1}{2} \delta \mathbf{x}_a + \frac{1}{2} \delta \mathbf{x}_b. \quad (5)$$

The work of the center of movable pulley can be expressed as

$$\mathbf{w} = \mathbf{w}_a + \mathbf{w}_b = \mathbf{f} \delta \mathbf{x}. \quad (6)$$

By applying Eq. (4) to Eq. (6), we can obtain the following equations:

$$\mathbf{f}_a \delta \mathbf{x}_a + \mathbf{f}_b \delta \mathbf{x}_b = \mathbf{f} \delta \mathbf{x}, \quad (7)$$

$$\mathbf{f} = \frac{\mathbf{f}_a \delta \mathbf{x}_a + \mathbf{f}_b \delta \mathbf{x}_b}{\delta \mathbf{x}}. \quad (8)$$

Also, by applying Eq. (5) to Eq. (8), we can get the resultant force and displacement equations at the movable pulley:

$$\delta \mathbf{x} = \frac{\delta \mathbf{x}_a + \delta \mathbf{x}_b}{2} \quad (9)$$

$$\mathbf{f} = 2 \frac{\mathbf{f}_a \delta \mathbf{x}_a + \mathbf{f}_b \delta \mathbf{x}_b}{\delta \mathbf{x}_a + \delta \mathbf{x}_b} \quad (10)$$

Now, by replacing the infinitesimal displacements with the corresponding velocity components, above Eq. (9) and Eq. (10) are rewritten as follows:

$$\mathbf{v} = \frac{\mathbf{v}_a + \mathbf{v}_b}{2} \quad (11)$$

$$\mathbf{f} = 2 \frac{\mathbf{f}_a \mathbf{v}_a + \mathbf{f}_b \mathbf{v}_b}{\mathbf{v}_a + \mathbf{v}_b} \quad (12)$$

Fig. 5 shows a typical speed-force characteristic of a conventional DC electric motor. In this paper, the motor is assumed to be operated in the continuous operation region. Fig. 6 shows the characteristics of DuMP calculated by Eq. (11) and Eq. (12). In this figure, (I) region is the speed-force characteristic of motor with low gear reduction, (II) region is the speed-force characteristic of motor with high gear reduction, and (III) lines are the combined speed-force characteristic that results from the DuMP. In other words, the speed-force characteristic of (III) lines implies the combined operating range of DuMP. To deal with the combined operating range easily, we will define a function $\Omega(F_{LOAD})$ which gives the maximum velocity as an output when a load force F_{LOAD} is applied to the DuMP. This will be utilized later and this is referred to as an *M-func* in this paper

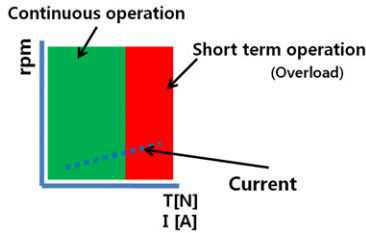


Fig. 5 Operating Range of Motor (RPM-Torque).

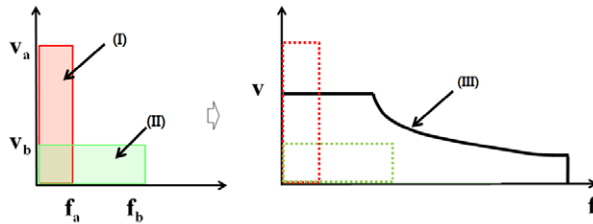


Fig. 6. The speed-force characteristic of the DuMP.
(a) Input characteristic, (b) Output characteristic.

Here, let us consider kinematics of the DuMP as shown in Fig. 4(a) and (b). The kinematic relation between joint angles of motors and displacement/angle of a movable pulley are described as following forms:

$$\mathbf{x} = \frac{1}{2} \mathbf{e}_a \mathbf{q}_a + \frac{1}{2} \mathbf{e}_b \mathbf{q}_b \quad (13)$$

$$\alpha = \frac{1}{2r} \mathbf{e}_a \mathbf{q}_a - \frac{1}{2r} \mathbf{e}_b \mathbf{q}_b$$

where \mathbf{e}_a and \mathbf{e}_b are the conversion rates that are products of gear reduction ratio and pulley radius, respectively. Now if we take the time derivative, then, we can get the velocity relation as follow:

$$\begin{bmatrix} \dot{\mathbf{x}} \\ \dot{\alpha} \end{bmatrix} = \begin{bmatrix} \frac{1}{2} \mathbf{e}_a & \frac{1}{2} \mathbf{e}_b \\ \frac{1}{2r} \mathbf{e}_a & -\frac{1}{2r} \mathbf{e}_b \end{bmatrix} \begin{bmatrix} \dot{\mathbf{q}}_a \\ \dot{\mathbf{q}}_b \end{bmatrix} \quad (14)$$

Above equation can be expressed as following compact form:

$$\dot{\mathbf{u}} = \mathbf{J} \dot{\mathbf{q}} \quad (15)$$

where \mathbf{J} is a Jacobian matrix. In this system, a rotation angle of pulley does not affect the movement of DuMP. Here, we consider only the position of movable pulley, \mathbf{x} , as an output variable which is controlled by using two input variables. Thus, the DuMP has one kinematic redundancy and Eq. (13), Eq. (14) are rewritten as

$$\mathbf{x} = \frac{1}{2} \mathbf{e}_a \mathbf{q}_a + \frac{1}{2} \mathbf{e}_b \mathbf{q}_b \quad (16)$$

$$\begin{bmatrix} \dot{\mathbf{x}} \end{bmatrix} = \begin{bmatrix} \frac{1}{2} \mathbf{e}_a & \frac{1}{2} \mathbf{e}_b \end{bmatrix} \begin{bmatrix} \dot{\mathbf{q}}_a \\ \dot{\mathbf{q}}_b \end{bmatrix} \quad (17)$$

Eq.(17) can be also expressed as following compact form:

$$\dot{\mathbf{x}} = \mathbf{J}_a \dot{\mathbf{q}} \quad (18)$$

Finally, let us obtain the general solution of Eq. (18) like this:

$$\dot{\mathbf{q}} = \mathbf{J}_a^+ \dot{\mathbf{x}} + (\mathbf{I} - \mathbf{J}_a^+ \mathbf{J}_a)(-\varepsilon) \frac{\partial \mathbf{P}}{\partial \mathbf{q}} \quad (19)$$

where $\dot{\mathbf{q}}$, $\dot{\mathbf{x}}$ and \mathbf{J}_a denote the input velocity vector, output velocity vector, and the Jacobain of kinematically redundant system, respectively[9][10]. The constant ε is a positive value, which can be determined arbitrarily based on the given task. Here, the control algorithm for each motor is carried out by using the homogeneous solution described by the second term of above equation. If the DuMP is operated for a long time, tendon wire around one side may be loosened. To prevent this situation, the rotation angle of pulley should be minimized without affecting the position of movable pulley, \mathbf{x} . Now, the performance index to be minimized is defined as

$$\mathbf{P} = (\alpha - 0)^2 = \left(\frac{1}{2r} \mathbf{e}_a \mathbf{q}_a - \frac{1}{2r} \mathbf{e}_b \mathbf{q}_b \right)^2 \quad (20)$$

As a result, we are able to control not only the position of the pulley (output variable of the DuMP) but also the length of the wire (internal variable) to prevent the wire from being released freely.

C. DuMP-SEA

The speed-force characteristic of DuMP can be extended

satisfying the three conditions mentioned in the previous section. Fig. 7 depicts the extended speed-force characteristics of the suggested DuMP-SEA (dashed line (I)) by using the energy stored in the spring, in which the solid line (II) expresses the characteristic of DuMP itself. In this figure, T_n is a pre-action time required to store the energy in the spring, $F_{s,n}$ is the stored spring force during the pre-action time and, at the same time, the released instant spring force when being released. And V_c is the maximal velocity of DuMP system. In other words, when the displacement of linear actuator decreases during pre-action time, the stored spring energy increases. Using the stored energy during pre-action time, M -func is extended like the property of SEA[1]. As a result, the suggested DuMP-SEA has not only advantage of DuMP such as high-speed and large-force, but also advantage of SEA obtained by using storage spring force at instance.

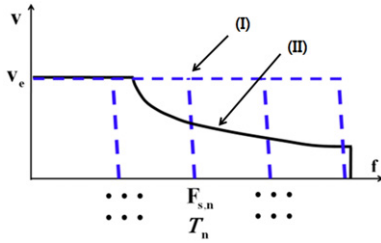


Fig. 7. Extended Speed-Force Characteristic of DuMP-SEA.

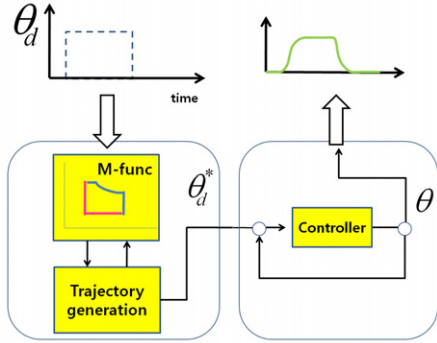


Fig. 8. Trajectory Generation.

III. TRAJECTORY GENERATION METHOD

This section explains a trajectory generation method of the suggested DuMP-SEA with 1 DOF as shown in Fig. 2. The trajectory generation method to quickly satisfy the desired angular displacement within the allowable performance range of DuMP is required as shown in Fig. 8. In previous section, since the M -func implies the allowable speed-force range of DuMP, we make use of the M -func to generate the available desired trajectory of angular displacement. More detail, the operation speed of DuMP must be limited according to loading force exerted on the DuMP. This can be realized using the function $\Omega(F_{LOAD})$ which gives the maximum velocity as an output when a load force F_{LOAD} is applied to the

DuMP. In other words, for given F_{LOAD} , we can get the allowable maximum speed by the function $\Omega(F_{LOAD})$. Ultimately, we can get the desired trajectory of angular displacement through the numerical integration of speed. Through these procedures, we can get the smooth desired trajectory of angular displacement as shown in Fig. 8.

IV. SIMULATION AND EXPERIMENT

Firstly, we assume that two identical motors are used for simulations and experiments, the simulations of DuMP are implemented with various gear ratios. Also, by operating a real DuMP and a real DuMP-SEA as shown in Fig. 1, the effectiveness of the suggested methods is verified through experiments.

A. Simulation

Fig. 9.(a) shows the 1DOF simulation model. Here, the pre-action to store spring energy gets started at 1[s] and the released time is 6[s]. Also, the corresponding desired set-point θ_d is 140° at 1[s] and 0° at 6[s], respectively. The desired trajectory $\theta_d^*(t)$ is generated in such a way to satisfy the M -func as suggested in the previous section. The displacement of DuMP, x , is controlled by the desired angular displacement, $\theta_d^*(t)$, and the spring force stored or released, f_s , is exactly proportional to $\theta_d^*(t)$.

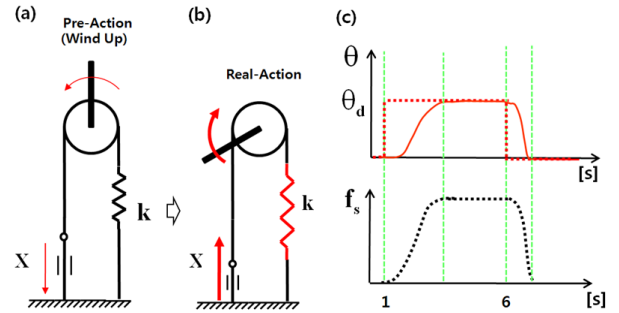


Fig.9. 1-DOF Simulation Model,

1) Case 1: DuMP-SEA, Motor- A (20:1) Motor- B(80:1)

Two 6.0[W] motors (continuous max. torque 6.77[mNm] and continuous max. speed 1000 [RPM]) are used for the simulation. All conditions are made identical to compare simulation results under various load force (F_{LOAD}) conditions. Here, four spring constants are chosen as four steps, such as $1/4*11000$ [N/m] $1/2*11000$ [N/m], $3/4*11000$ [N/m] and 11000 [N/m], for four simulations. Fig. 10 shows the speed-force characteristics (M -func) of the case 1. Fig. 11 is the simulation results. As shown in Fig 11.(a), the small load force (line(I), $k = 11000*1/4$) in pre-action (wind up) shows the maximum speed to approach the set-point θ_d . Also, the large load force (line(II), $k = 11000$) in pre-action (wind up) shows that θ quickly increases at the beginning but slows down at the latter part because of the operation region of

M-func. All simulation results satisfy the given *M-func* range as shown in Fig. 11.(c).

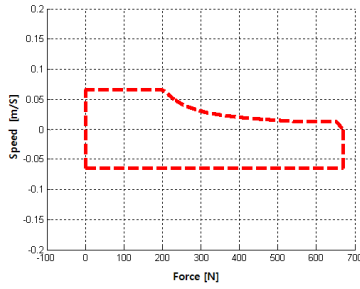


Fig.10. Speed – Force characteristic (*M-func*) of the Case 1.

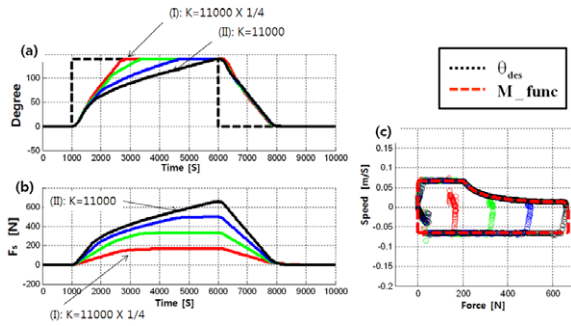


Fig.11. Simulation Results of Case 1.

2) Case 2: DuMP-SEA , Motor- A (4:1), Motor- B(80:1)

In the second simulation, the spring constants are newly chosen as four steps such as $1/4 \times 8800$ [N/m], $1/2 \times 8800$ [N/m], $3/4 \times 8800$ [N/m] and 8800 [N/m] for four simulations. The *M-func* as shown in Fig. 12 shows the increased speed region thanks to the lowered gear reduction ratio of the motor-A compared to Fig. 10.

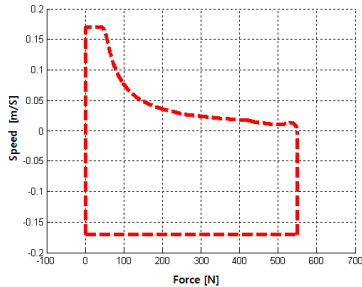


Fig.12. Speed – Force characteristic (*M-func*).

Fig. 13 shows the simulation results of case 2. The small load force (line(I), $k = 1/4 \times 8800$) case approaches quicker to the set-point θ_d than case 1. However, when the load force becomes larger as shown in lines(II), (III), (IV), the pre-action takes much time and is slower than case 1. Also, we can see that all simulation results satisfy the given *M-func* range as shown in Fig. 13.(c).

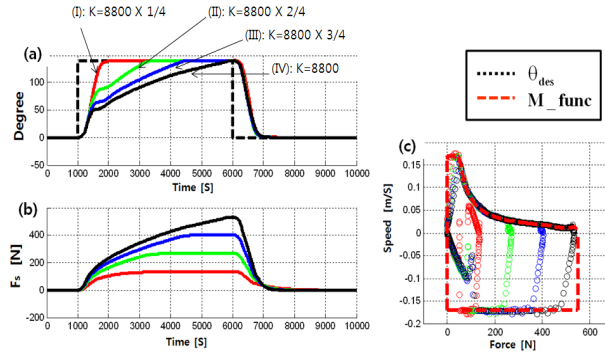


Fig.13. Simulation Results of Case 2.

3) Case 3 : Conventional SEA - Single Motor (4:1)

The motor is assumed to have two-times power (12.0[W]) of motor compared to the case 1 and 2 (6.0[W]). And the spring constants are the same as the case 2.

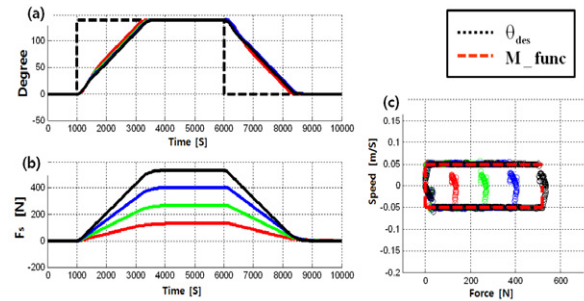


Fig.14. Simulation Results of Case 3.

Fig. 14 shows the simulation results. As shown in Fig. 14.(a), though the different spring constants are used for simulations, the pre-action takes almost same time. This does not offer a variety of speed-force characteristics differently from the DuMP of cases 1 and 2. Also, we can see that all simulation results satisfy the given *M-func* range as shown in Fig. 14.(c).

B. Real DuMP-SEA, Motor A (1:1), Motor B (5:1)

To verify the applicability of the real-hardware, we made a prototype DuMP-SEA system. The prototype of DuMP-SEA consists of low cost motors with 4 pulses encoder per one rotation. In addition, we make use of an absolute encoder to measure the position of the link and the DSP (TMS320F2406) as a control system. In this experiment, the motor-A and B are operated by PWM driven method. For performance comparison, we assume that 100% duty-cycle is applied to the motor-A and 50% duty-cycle is applied to the motor-B. The Fig. 15.(a) shows the behavior of DuMP-SEA according to the change of load force. In there, line (I) shows when the spring constant is 80 [Nm] and line (II) shows when two-times spring constant (160[Nm]) is applied. Also, we can see that the released speeds of two cases are almost the same. As shown in Fig 15.(a), the small load force (line(I), $k = 80$ [N/m]) in pre-action (wind up) shows the fast speed to approach the set-point θ_d . On the contrary, the large load force

(line(II), $k = 160$) shows that θ quickly increases at the beginning but slows down at the latter part, similarly with the previous simulation results. In addition, we can make the slow motion pattern as well as the fast motion by adjusting the duty-cycle of PWM input as shown in Fig. 15.(b). As a result, we could confirm the applicability of the suggested DuMP system for practical use.

C. Experimental Results

Previous simulation results have shown the existence of *M-func* region and the time taken to move to the desired set-point as the pre-action differs according to the load forces (spring constants). The energy stored in the spring during pre-action was utilized for the maximum speed of *M-func* at the released time. In addition, we have shown that the prototype of DuMP-SEA also operates in accordance to the simulation. The Fig. 16 shows the extended *M-func* of DuMP-SEA according as the pre-action time increases.

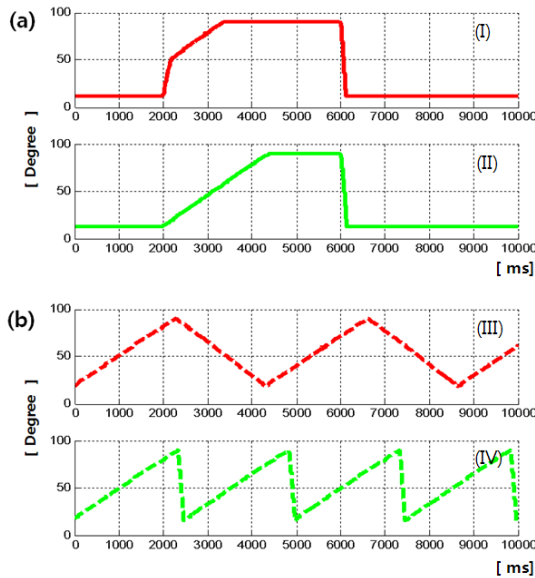


Fig.15. Experimental Results of Real DuMP-SEA.

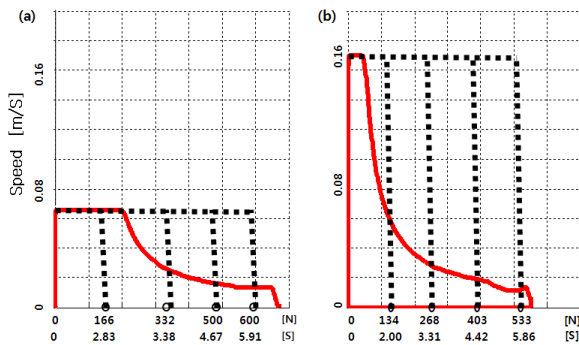


Fig.16. Extended *M-func*.

(a) Simulation of Case 1 (b) Simulation of Case 2.

In order to operate the suggested DuMP-SEA up to 500[N], approximately 4.8[s] and 5.8[s] for pre-action are required for case 1 and 2, respectively. When comparing case 1 and 2,

case 1 is advantageous in terms of pre-action time and case 2 has advantage of faster movement. Lastly, we have shown that both high speed and large force could be generated by the suggested new actuator system (DuMP-SEA), even though small motors were utilized for the DuMP.

V. CONCLUDING REMARKS

The Dual-motors actuator system using a Movable Pulley (DuMP) has been designed and analyzed in this paper. Also, the DuMP was applied to the conventional SEA system (DuMP-SEA). Through simulations and experiments, we have shown the validity of the suggested DuMP-SEA, which is able to offer the high speed and large force to the bio-mimetic system and rehabilitation robots. Also, the suggested actuator mechanism was very simple in the mechanical structure. Also, the suggested would be able to softly contact to the human because the suggested could be made as a form of light-weighted, compact-sized and safety-assured system. For future works, we are planning to design elaborate hardware system and to apply to wearable robots or rehabilitation robots.

REFERENCES

- [1] J. K. Hitt, M. A. Oymagil, T. G. Sugar, K. W. Hollander, A.W. Boehler, and J. Fleeger, "Dynamically Controlled Ankle Foot Orthosis (DCO) With Regenerative Kinetics: Incrementally Attaining User Portability," *IEEE International Conference on Robotics and Automation*, 2007.
- [2] J.Naito, G.Obinata, A.Nakayama, and K. Hase, "Development of a Wearable Robot for Assisting Carpentry Workers," *International Journal of Advanced Robotic Systems*, Vol. 4, No. 4, pp. 431-436, 2007.
- [3] D. P. Ferris, J. M. Czerniecki, B. Hannaford, "An Ankle-Foot Orthosis Powered by Artificial Muscles," *Journal of Applied Biomechanics*, Vol. 21, pp. 189-197, 2005.
- [4] H. Vallery, J. Veneman, E. Asseltonk, R. Ekkelenkamp, M. Buss, AND H. Kooij, "Compliant Actuation of Rehabilitation Robots," *IEEE Robotics and Automation Magazine*, Vol. 15, No.3 September, 2008.
- [5] A. Schaffer, O. Eiberger, M. Grebenstein, S. Haddadin, C. Ott,T. Wimbock, S. Wolf, and G. Hirzinger, "SoftRobotics," *IEEE Robotics and Automation Magazine* Vol. 15, No.3 September, 2008.
- [6] U. Scarfogliero, C. Stefanini, P. Dario, "Design and Development of the Long-Jumping "Grillo" Mini Robot," *IEEE International Conference on Robotics and Automation*, pp. 10-14 April 2007.
- [7] T. G. Sugar, "A Novel Selective Compliant Actuator," *Journal of Mechatronics*, Vol. 12, No. 9, November 2002.
- [8] G. A. Pratt and M. M. Williamson, "Series elastic actuators," *IEEE/RSJ International Conference on Intelligent Robots and Systems*. Pittsburg, pp. 399-406, July, 1995.
- [9] H. Lee, B.-J. Yi, S. R. Oh, and I. H. Suh, "Optimal Design and Development of a Five-bar Finger with Redundant Actuation," *Mechatronics*, Vol. 11, No. 1, pp. 27-42, 2001.
- [10] B.-J. Yi and W.K. Kim, "Optimal design of a redundantly actuated 4-legged 6 degree of freedom manipulator using composite design index," *KSME International Journal*, Vol. 8, No. 4, pp. 385-403, 1994.